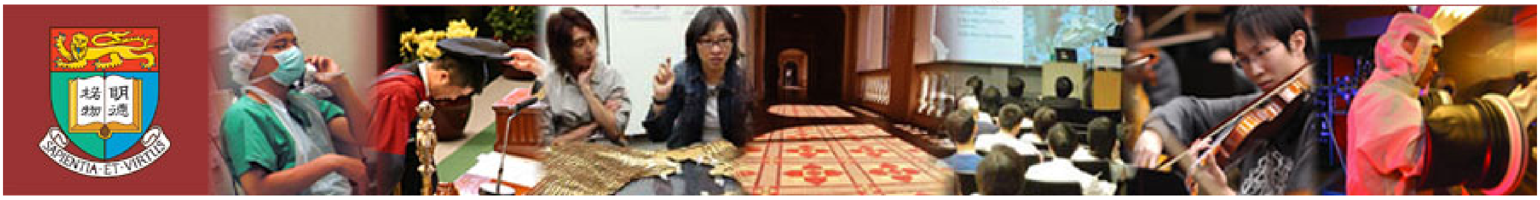

Title	Electronic transitions of iridium monoboride
Author(s)	Pang, HF; Ng, YW; Xia, Y; Cheung, ASC
Citation	Chemical Physics Letters, 2011, v. 501 n. 4-6, p. 257-262
Issued Date	2011
URL	http://hdl.handle.net/10722/134347
Rights	NOTICE: this is the author's version of a work that was accepted for publication in Chemical Physics Letters. Changes resulting from the publishing process, such as peer review, editing, corrections, structural formatting, and other quality control mechanisms may not be reflected in this document. Changes may have been made to this work since it was submitted for publication. A definitive version was subsequently published in Chemical Physics Letters, 2011, v. 501 n. 4-6, p. 257-262. DOI: 10.1016/j.cplett.2010.11.084

Elsevier Editorial System(tm) for Chemical Physics Letters
Manuscript Draft

Manuscript Number: CPLETT-10-2055R1

Title: Electronic transitions of iridium monoboride

Article Type: Regular Article

Section/Category: Gaseous Molecules

Corresponding Author: Dr. Allan Cheung, Ph.D

Corresponding Author's Institution: University of Hong Kong

First Author: Hon F Pang, M.Sc.

Order of Authors: Hon F Pang, M.Sc.; Y W Ng, B.Sc.; Ye Xia, B.Sc.; Allan Cheung, Ph.D

Abstract: Electronic transitions spectrum of iridium monoboride in the spectral region between 400 and 545nm has been recorded and analyzed using laser vaporization/reaction free jet expansion source and laser induced fluorescence spectroscopy. Thirteen vibrational bands belonging to four electronic transitions, namely the [18.8] 3DEL3 - X3DEL3, [21.1] 3PHI4 - X3DEL3, [22.8] 3PHI3 - X3DEL3, and [22.4] 1PHI3 - a1DEL2 transitions, have been identified and rotationally analyzed. Spectra of all four isotopic molecules were observed.

Research Highlights:

. New molecular transition bands of IrB

. Four new electronic transitions have been observed and analyzed

. Molecular constants of the upper and lower states were determined

***Graphical Abstract (pictogram)**

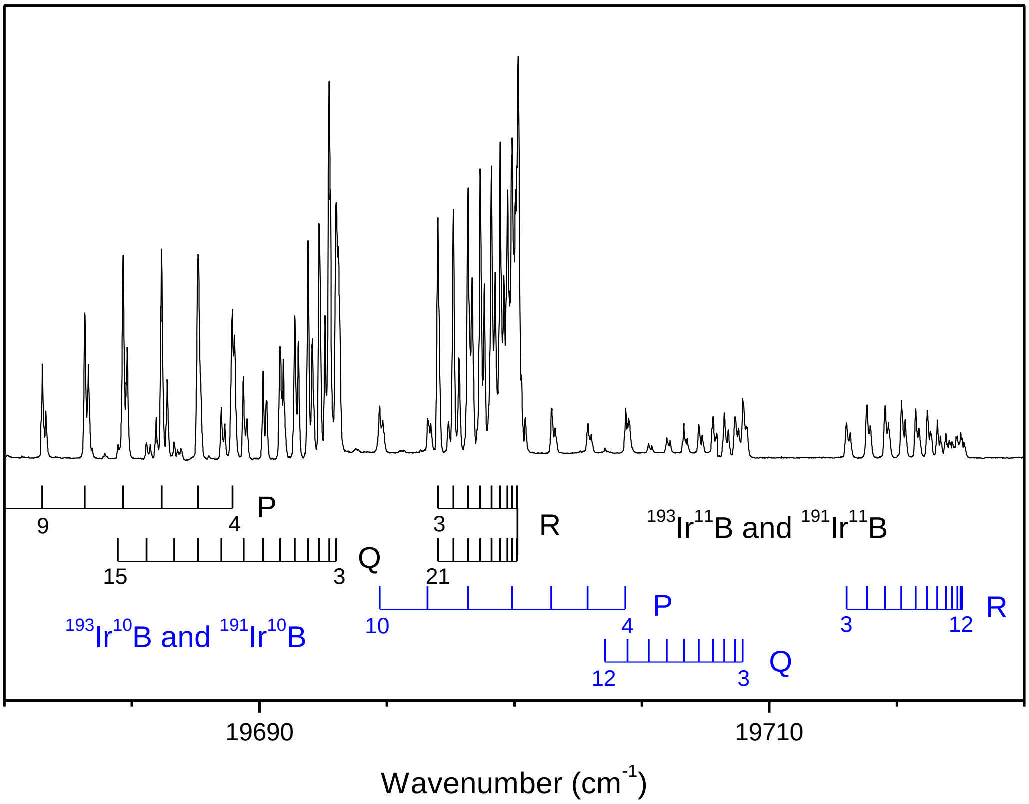

Electronic transition spectrum of the (1, 0) band of the [18.8] $^3\Delta_3 - X^3\Delta_3$ system of IrB with all four isotopic molecules resolved

Electronic transitions of iridium monoboride

H.F. Pang, Y.W. Ng, Y. Xia and A.S-C. Cheung*

Department of Chemistry, The University of Hong Kong, Pokfulam Road, Hong Kong

Proposed running head: Electronic transitions of IrB

*Correspondence to:

Prof. A.S.C. Cheung
Department of Chemistry
The University of Hong Kong
Pokfulam Road
Hong Kong

Tel : (852) 2859 2155
Fax : (852) 2857 1586
Email : hrsccsc@hku.hk

Text	:	12
Tables	:	2
Figures	:	6

ABSTRACT

Electronic transitions spectrum of iridium monoboride in the spectral region between 400 and 545nm has been recorded and analyzed using laser vaporization/reaction free jet expansion source and laser induced fluorescence spectroscopy. Thirteen vibrational bands belonging to four electronic transitions, namely the [18.8] $^3\Delta_3$ – $X^3\Delta_3$, [21.1] $^3\Phi_4$ – $X^3\Delta_3$, [22.8] $^3\Phi_3$ – $X^3\Delta_{3,}$ and [22.4] $^1\Phi_3$ – $a^1\Delta_2$ transitions, have been identified and rotationally analyzed. Spectra of all four isotopic molecules were observed.

I. INTRODUCTION

Metal borides (MB) are characterized by a great number of unique properties[1]. Most of the borides are refractory material with melting points above 2000K, high hardness and excellent conductivity. Recently, there were reports on super-hardness properties of the rhenium boride (ReB_2) bulk[2] and rhodium (RhB) and iridium (IrB) films[3]. The electrical conductivity of titanium diboride (TiB_2) is known to be five times better than the titanium metal itself[4]. In addition, magnesium diboride (MgB_2) was found to have superconductivity at 39K[5]. Despite of all these important properties that have been found in MB, experimental study of MB molecules is very limited.

Iridium containing species have long been an interesting research topic because of their importance in iridium based alloys[6] and also in catalytic processes involving the activation and formation of carbon bonds (X = H, C, O, F etc.)[7,8]. Spectroscopic properties of diatomic molecules formed with Ir and main group elements of the 2p period have recently been investigated, which include IrB[9], IrC[10], IrN[11], IrO[12], and IrF[13]. For iridium monoboride (IrB), our group using laser induced fluorescence spectroscopy recorded vibrational bands of electronic transition in the visible region between 545nm and 610nm, identified the ground $X^3\Delta_3$ state, and reported the $[16.5]^3\Pi_2 - X^3\Delta_3$ transition. Molecular parameters including hyperfine constants of the $^3\Pi_2$ and $^3\Delta_3$ states studied were determined.[9]

In this work, we report the analysis of thirteen vibrational bands belonging to four electronic transitions recorded using the technique of laser vaporization reaction free jet expansion and laser induced fluorescence (LIF) spectroscopy. Spectra of all the four isotopes: $^{191}Ir^{10}B$, $^{193}Ir^{10}B$, $^{191}Ir^{11}B$ and $^{193}Ir^{11}B$ were resolved and studied.

II. EXPERIMENT

The experimental apparatus and detailed procedures for producing metal containing molecules using laser vaporization/reaction free-jet expansion source and LIF spectroscopy have been described in earlier publication.[14] Only a brief description of the relevant experimental conditions for obtaining IrB spectrum is given here. Frequency-doubled Nd:YAG laser pulses with 5-6 mJ were focused onto the surface of an iridium rod to generate iridium atoms. A pulsed valve was synchronized with appropriate time delay released gas mixture of 0.5% B_2H_6 in argon to react with the iridium atoms for the production of IrB. A pulsed dye laser operated with Coumarin dyes and pumped by a Nd:YAG laser with wavelength set to 355nm produced tunable output in the visible region, which was used to excite the IrB molecules produced. The LIF signal was collected by means of a lens system and detected by a photomultiplier tube (PMT). The PMT output was fed to a fast oscilloscope for averaging and storage. The laser linewidth of the tunable dye laser was about 0.07cm^{-1}. However, typical molecular linewidth obtained was larger than 0.1cm^{-1}, which is likely to be due to unresolved hyperfine structure in the rotational lines.

III. RESULTS AND DISCUSSION

A. Low Resolution Broadband Spectrum

Low resolution LIF spectrum of IrB in the spectral region between 400 to 545nm has been recorded. A broadband scan of the IrB spectrum is shown in Figure 1, which shows three transition systems. A total of 13 transition bands were recorded and analyzed. We were able to identify four electronic transitions, namely the [18.8] $^3\Delta_3$ – $X^3\Delta_3$, [21.1] $^3\Phi_4$ – $X^3\Delta_3$, [22.8] $^3\Phi_3$ – $X^3\Delta_{3,}$ and [22.4] $^1\Phi_3$ – $a^1\Delta_2$ transitions. Except the [22.4] $^1\Phi_3$ – $a^1\Delta_2$ transition, all other three transitions originate from the ground $X^3\Delta_3$ state. As far as the least squares fitting of the molecular lines were concerned, for those lines originated from the ground $X^3\Delta_3$ state the rotational constant B was fixed at value determined earlier[9]. Figure 2 summarizes the electronic transitions identified and studied so far. Individual electronic transition observed is discussed in detail below. A list of the measured line positions of all the recorded transitions is deposited in the journal archive.

B. The [18.8]$^3\Delta_3$ – $X^3\Delta_3$ Transition

We have recorded three vibrational bands of this system: the (0, 0), (1, 0) and the (1, 1) bands. Figure 3 shows the (1, 0) band with all four isotopic molecules. The assignment of rotational structure was straight forward. The P, Q, and R branches are clearly resolved; from their respective first lines, namely P(4), Q(3) and R(3), we concluded that the upper state of this transition has an $\Omega = 3$ value. The intensity of the P and R branches is generally strong, which is consistent with a $\Delta\Lambda = 0$ transition. The upper state is assigned to be $^3\Delta_3$ state. The observed line positions were fit to the following expression:

$$\nu = \nu_o + B'J'(J' + 1) - D'[J'(J'+1)]^2 - \{B''J''(J'' + 1) - D''[J''(J''+1)]^2\}, \qquad (1)$$

where $'$ and $''$ refer to the usual rotation for the upper and the lower states, respectively. ν_o is the band origin, and B and D are the rotational and centrifugal distortion constants. Since only low J ($J < 12$), lines were measured. In the least squares fit, the centrifugal distortion constant was set to zero. Molecular constants obtained for the [18.8] $^3\Delta_3$ state are listed in Table 1. The $\Delta G_{1/2}$ value determined for the [18.8] $^3\Delta_3$ and the $X^3\Delta_3$ states are 931.88 and 909.64 cm^{-1} respectively for the most abundant $^{193}Ir^{11}B$ isotope.

C. The [21.1] $^3\Phi_4 - X^3\Delta_3$ Transition

Five vibrational bands of this electronic transition including the (v, 0) with v = 0 - 3 and the (0, 1) band were observed and analyzed. Fig. 4 shows the (1, 0) band with well resolved P, Q and R branches. The first line of the respective branches are R(3), Q(4), and P(5), which established unambiguously the upper state has an $\Omega = 4$ value. The intensity of the R and Q branches are much larger than the P branch, which is consistent with a transition with $\Delta\Lambda = +1$. The upper state is, therefore, assigned as [21.1]$^3\Phi_4$ state. Least squares fit results of this transition is listed in Table 1. Again in this transition, all four isotopes were observed and analyzed. The $\Delta G_{1/2}$ of the $X^3\Delta_3$ state of the $^{193}Ir^{11}B$ isotope was determined to be 909.63cm^{-1}, which agrees extremely well with the value determined from that of the [18.8] $^3\Delta_3 - X^3\Delta_3$ transition.

D. The [22.8] $^3\Phi_3 - X^3\Delta_3$ Transition

Three vibrational bands (v, 0) with v = 0 – 2 of this electronic transition were recorded and analyzed. Fig 5 depicts the (2, 0) band of this transition. The first line of the P, Q and the R branches are with J value equal to 4, 3 and 3 respectively, which indicate that the upper state is with an $\Omega = 3$ value. The intensity of the R and Q branches are stronger than the P branch, the upper state is, therefore, assigned as [22.8] $^3\Phi_3$ state. This transition is generally weaker than other transitions. We only obtained spectrum of the ^{191}Ir^{11}B and ^{193}Ir^{11}B molecules. Molecular constants obtained from fitting the rotational lines are listed in Table 1.

E. The [22.4] $^1\Phi_3 – a^1\Delta_2$ Transition

We recorded the (0, 0) and (1, 0) bands with heads at 22440 and 23128 cm^{-1} respectively. The (0, 0) band of this transition is shown in Fig 6. Assignment of rotational lines was straight forward. The first line of the branches are R(2), Q(3), and P(4), which indicates that the $\Omega' = 3$ and $\Omega'' = 2$. In addition, as shown in Fig. 6 the R and Q branches are stronger than the P branch, which is consistent with a $\Delta\Lambda = +1$ transition. The low resolution spectrum in Fig. 1 shows clearly that the two vibrational bands in this system are stronger in intensity than those other transitions originated from the same $X^3\Delta_3$ state. We have also recorded the resolved fluorescence spectrum of these bands. The vibrational separation of the lower state with $\Omega'' = 2$ is about 1018 ± 25 cm^{-1}, which is very different from the 909 cm^{-1} of the $X^3\Delta_3$ state. As far as the assignment of the lower state of this transition is concerned, we have considered the possibilities of $\Omega = 2$ of the $X^3\Delta$ state or of the $a^1\Delta$ state. We noticed that the spin-orbit of the Ir atom is very large and in the order of 2000 – 4000 cm^{-1} [15], IrB molecule formed would also be expected to have spin-orbit components in the order of thousands of wavenumbers. Therefore, the Ω = 2 component is expected to be located at much higher energy than the lowest Ω = 3 component of the $X^3\Delta$ state and the population of the Ω = 2 component should be very low when compares to the ground state. In addition, the rotational constant for the $X^3\Delta_3$ state is 0.5181 cm^{-1}, which is relatively larger than that of our determined $\Omega'' = 2$ level with a value of 0.5153 cm^{-1}. Based on the differences in transition intensity (the $a^1\Delta_2$ is a metastable state), vibrational separations and rotational constants mentioned above, we assigned the lower state of this transition to be the $a^1\Delta_2$ state. Consequently, the upper state is assigned as $^1\Phi_3$ state. The molecular constants obtained from the least squares fit of the observed lines for the two states are also listed in Table 1.

The four IrB isotopes are $^{191}Ir^{10}B$, $^{193}Ir^{11}B$, $^{191}Ir^{11}B$, and $^{193}Ir^{11}B$ and their relative natural abundance are respectively 0.15 0.25 0.59 and 1. Molecular parameters for the isotopic molecules are related by different powers of the mass dependence parameter $\rho = (\mu/\mu_i)$ when μ and μ_i are the reduced mass of an isotope and its heaviest isotope $^{193}Ir^{11}B$. The agreement between molecular constants of the four isotopes is excellent and, generally, with uncertainty in the range of one standard deviation of the molecular constants determined. It is because the vibrational separations of the excited states are to some extent shifted by unknown perturbation; it may not be useful or helpful to tabulate the equilibrium molecular constants.

F. Discussion

The ground of IrB as discussed in Ref. 9 is:

$(1\sigma)^2\ (1\pi)^4\ (1\delta)^3\ (2\sigma)^1 \quad \rightarrow \quad X^3\Delta_i$ and a $^1\Delta_2$

Table 2 lists the many low-lying excited electronic states arisen from excited electronic configurations with only one electron jump from the ground electronic configuration (Label A). Many of the triplet states listed in the table are formed from molecular orbital (MO) with δ^3 or π^3 occupation, therefore, they are inverted states with the largest Ω value having the lowest energy. It is well known that the iridium atom has large spin-orbit interaction and molecules formed from iridium would generally have large spin-orbit splitting, and hence, the spin components with different Ω values would be quite far apart. In such situation, the spin components should better be described using Hund's case (c) coupling scheme[16]. In this work, using single electronic configuration approach, the electronic transition observed can be considered as the promotion of an electron from the ground state to the excited state with different electronic configurations. The $[16.5]^3\Pi_2 - X^3\Delta_3$, $[21.1]\ ^3\Phi_4 - X^3\Delta_3$ and $[22.8]\ ^3\Phi_3 - X^3\Delta_3$ systems transition can be considered as the promotion of an electron from the 2σ orbital (Label A) to the 2π orbital (Label D). The difference between the band origins of the $[21.1]^3\Phi_4$ and $[22.8]^3\Phi_3$ states is about 1622 cm^{-1}, it is reasonable that these states are the Ω = 3 and Ω = 4 components of the same inverted $^3\Phi_i$ state. This assignment is consistent with the observation that the $[22.8]\ ^3\Phi_3 - X^3\Delta_3$ transition is weaker than the $[21.1]\ ^3\Phi_4 - X^3\Delta_3$ transition because the $\Delta\Lambda = \Delta\Omega = +1$ should be the stronger sub-band transition. In addition, the $[22.4]^1\Phi_3 - a^1\Delta_2$ transition would also arise from the promotion of an electron from the 2σ (Label A) also 2π orbital (Label D). However, the $[18.8]^3\Delta_3 - X^3\Delta_3$ transition observed can be considered as the promotion of an electron from the 2σ orbital (Label A) to the 3σ orbital (Label E). We have performed preliminary *ab initio* calculations on IrB and the $a^1\Delta$ state was calculated to be about 1500 cm^{-1} above the $X^3\Delta$ state[17]. A detailed theoretical computation with the level of theory down to individual spin-orbit components of each state will be really useful to confirm our assignments here.

The aim of this work is to study the upper electronic states of the IrB molecule; this task is getting more difficult because as we move up the energy scale, more and more states that could only be identified with the Ω value. This is due, on the one hand, partially to the sizeable spin-orbit interaction in the molecule and electronic states are practically in Hunds' case (c) coupling scheme, it is difficult to assign any Λ value to these sub-states. On the other hand, the relatively strong spectra of the $Ir^{10}B$ isotopic molecule are widely separated from the $Ir^{11}B$, for instance, the v = 2 level of the $[21.1]^3\Phi_3$ state the isotopic separation is over 28 cm^{-1}. Combining those with the situation that the separation between vibrational levels is very often irregular, it is rather difficult to link the spectra of isotopic molecules together. From our low resolution scan, we have observed numerous bands that are comparable in intensity, but it is difficult to identify any vibrational progressions. Similar excited state patterns have also been observed in the spectra of iridium containing molecules such as IrC[14], IrN[18] and also IrP[19].

Acknowledgements

The work described here was supported by a grant from the Research Grants Council of the Hong Kong Special Administrative Region, China. (Project numbers HKU 701008).

References:

1. Y.G. Gogotsi and R.A. Andrievski, “Materials Science of Carbides, Nitrides, and Borides”, *NATO Science Series* **Vol. 68**, Kluwer Academic Pub. 1999.
2. H. Chung, M.B. Weinberger, J.B. Levine, A. Kavner, J. Yang, S.H. Tolbert, and R.B. Kaner, *Science*, **316**, 436 (2007).
3. A. Latini, J.V. Rau, R. Teghil, A. Generosi, and V.R. Albertini, *App. Mater. Interfaces*, **2**, 581 (2010).
4. G. Will, *J. Solid State Chem.*, **177**, 628 (2004).
5. J. Nagamatsu, N. Nakagawa, T. Muranaka, Y. Zenitani, and J. Akimitsu, *Nature*, **410**, 63 (2001).
6. E.K. Ohrinu, R.D. Lanam, P. Panfilov, and H. Harada Eds, *Iridium-Procedings of the international symposium*, The Minerals Metals and Materials Society (2000).
7. M.A. Ciriano, L.A. Oro and M.T. Camellini. *Organometallics*, **14**, (1995) 4764.
8. R. Jimenez-Catano and M.B. Hall. *Organometallics*, **15** (1996), 1889.
9. J. Ye, H.F. Pang, A. M-Y. Wong, J.W-H. Leung, and A. S-C. Cheung, *J. Chem. Phys.*, **128**, 154321 (2008).
10. A. J. Marr, M. E. Flores, and T.C. Steimle, *J. Chem. Phys.*, **104**, 8183 (1996).
11. T.C. Steimle, A.J. Marr, S.A. Beaton, and J.M. Brown, *J. Chem. Phys.*, **106**, 2073 (1997).
12. K. Jansson, and R. Scullman, *J. Mol. Spectrosc.*, **43**, 208 (1972).
13. A.G. Adam, A.D. Granger, L.E. Downie, D.W. Tokaryk and C. Linton, *Can. J. Phys.*, **87**, 557 (2009).
14. H.F. Pang and A. S-C Cheung, *Chem. Phys. Lett.*, **471** (2009) 194.
15. J.E. Sausonetti, W.C. Martin, and S.L. Young. *Handbook of basic atomic spectroscopic data (version 1.1.2) National Institute of Standard and Technology*, Gaithensburg. M.D. U.S.A. 2005.
16. G. Herzberg, *Spectra of Diatomic Molecules*, Van Nostrand, New York, 1950.

17. A. S-C. Cheung, H.F. Pang, Y. W. Ng, and Guanghui Chen, 65th OSU International Symposium on Molecular Spectroscopy, June 2010, Columbus, Ohio, USA. Paper WF02.

18. H.F. Pang and A. S-C. Cheung, *Chin. J. Chem. Phys.*, **22**, 157 (2009).

19. H.F. Pang, A. Liu, Y. Xia, and A. S-C. Cheung, *Chem. Phys. Lett.* **494**, 155 (2010).

Table legends:

Table 1 Molecular Constants for the [18.8]$^3\Delta_3$, [21.1] $^3\Phi_4$, [22.8] $^3\Phi_3$, [a+22.4]$^1\Phi_3$, a$^1\Delta_2$ and X$^3\Delta_3$ states of IrB

Table 2 Electronic configuration of low-lying excited states of IrB

Figure captions:

Figure 1. Broadband spectrum of IrB between 431 and 454 nm.

Figure 2. Observed electronic transition systems of IrB

Figure 3. (1, 0) band of the [18.8] $^3\Delta_3$ – X$^3\Delta_3$ transition of IrB

Figure 4. (1, 0) band of the [21.1] $^3\Phi_4$ – X$^3\Delta_3$ transition of IrB

Figure 5. (2, 0) band of the [22.8] $^3\Phi_3$ – X$^3\Delta_3$ transition of IrB

Figure 6. (0, 0) band of the [22.4] $^1\Phi_3$ – a $^1\Delta_2$ transition of IrB

Table 1. Molecular constants for the $[18.8]^3\Delta_3$, $[21.1]\ ^3\Phi_4$, $[22.8]\ ^3\Phi_3$, $[a + 22.4]^1\Phi_3$, $a^1\Delta_2$ and $X^3\Delta_3$ states of IrB (cm^{-1})

State	Parameter	$^{193}Ir^{11}B$	$^{191}Ir^{11}B$	$^{193}Ir^{10}B$	$^{191}Ir^{10}B$
$[18.8]^3\Delta_3$	T_1	19693.51(2)	19693.64(3)	19709.33(2)	19709.46(2)
	B_1	0.4805(2)	0.4806(3)	0.5300(3)	0.5301(2)
	T_o	18761.63(2)	18761.64(2)	18759.86(3)	18759.86(3)
	B_o	0.5052(2)	0.5054(3)	0.5527(2)	0.5529(3)
$[21.1]\ ^3\Phi_4$	T_3	22554.49(4)	22554.57(3)	22580.81(3)	22580.92(3)
	B_3	0.4499(5)	0.4502(3)	0.4867(5)	0.4869(4)
	T_2	22158.00(6)	22158.26(6)	22186.30(6)	22186.57(5)
	B_2	0.4647(8)	0.4649(8)	0.5143(9)	0.5133(8)
	T_1	21650.29(5)	21650.33(5)	21661.64(8)	21661.71(8)
	B_1	0.4687(4)	0.4693(5)	0.5153(8)	0.5154(8)
	T_o	21159.37(5)	21159.42(4)	21153.98(3)	21154.00(2)
	B_o	0.4855(7)	0.4856(6)	0.5321(3)	0.5323(3)
$[22.8]\ ^3\Phi_3$	T_2	24292.27(4)	24292.79(4)		
	B_2	0.4506(5)	0.4523(5)		
	T_1	23541.03(1)	23541.31(1)		
	B_1	0.4595(1)	0.4597(1)		
	T_o	22781.22(6)	22781.23(6)		
	B_o	0.4692(8)	0.4695(8)		
$[a + 22.4]^1\Phi_3$	T_1	a + 23122.17(3)	a + 23122.63(4)		
	B_1	0.4668(6)	0.4683(8)		
	T_o	a + 22435.44 (2)	a + 22435.93(2)		
	B_o	0.4609(1)	0.4612(2)		
$a^1\Delta_2$	T_o	a	a		
	B_o	0.5153(2)	0.5156(3)		
$X^3\Delta_3$	T_1	909.63(2)	909.92(2)		
	B_1	0.5140(3)	0.5142(3)		
	T_o	0.000	0.000	0.000	0.000
	B_o*	0.51809	0.51839	0.56684	0.56713

Values given in parenthesis are one standard error in the last significant figure quoted

*Molecular constants from Ref. 9

Table 2. Electronic configurations of low-lying excited states of IrB

Label	Molecular Orbital Occupancies						Configuration	States
	1σ	1π	1δ	2σ	2π	3σ		
A	2	4	3	1			$\delta^3\sigma$	$X^3\Delta_i$,$a^1\Delta$
B	2	3	4	1			$\pi^3\sigma$	$^1\Pi$, $^3\Pi_i$
C	2	4	2	2			δ^2	$^3\Sigma^-$, $^1\Sigma^+$, $^1\Gamma$
D	2	4	3		1		$\delta^3\pi$	$^3\Phi_i$, $^3\Pi_i$, $^1\Phi$, $^1\Pi$
E	2	4	3			1	$\delta^3\sigma$	$^1\Delta$, $^3\Delta_i$

Figure 1

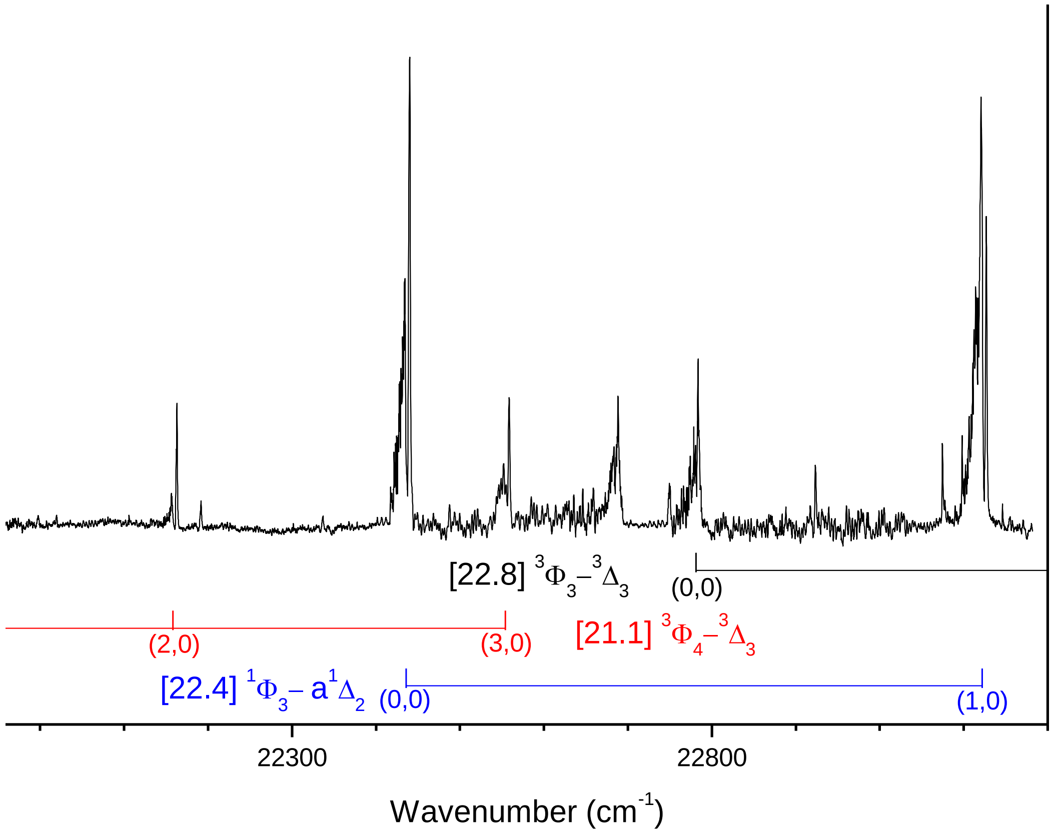
[22.8] $^3\Phi_3-^3\Delta_3$
(0,0)
(2,0)
(3,0)
[21.1] $^3\Phi_4-^3\Delta_3$
[22.4] $^1\Phi_3-a^1\Delta_2$
(0,0)
(1,0)
22300
22800
Wavenumber (cm^{-1})

Figure 2

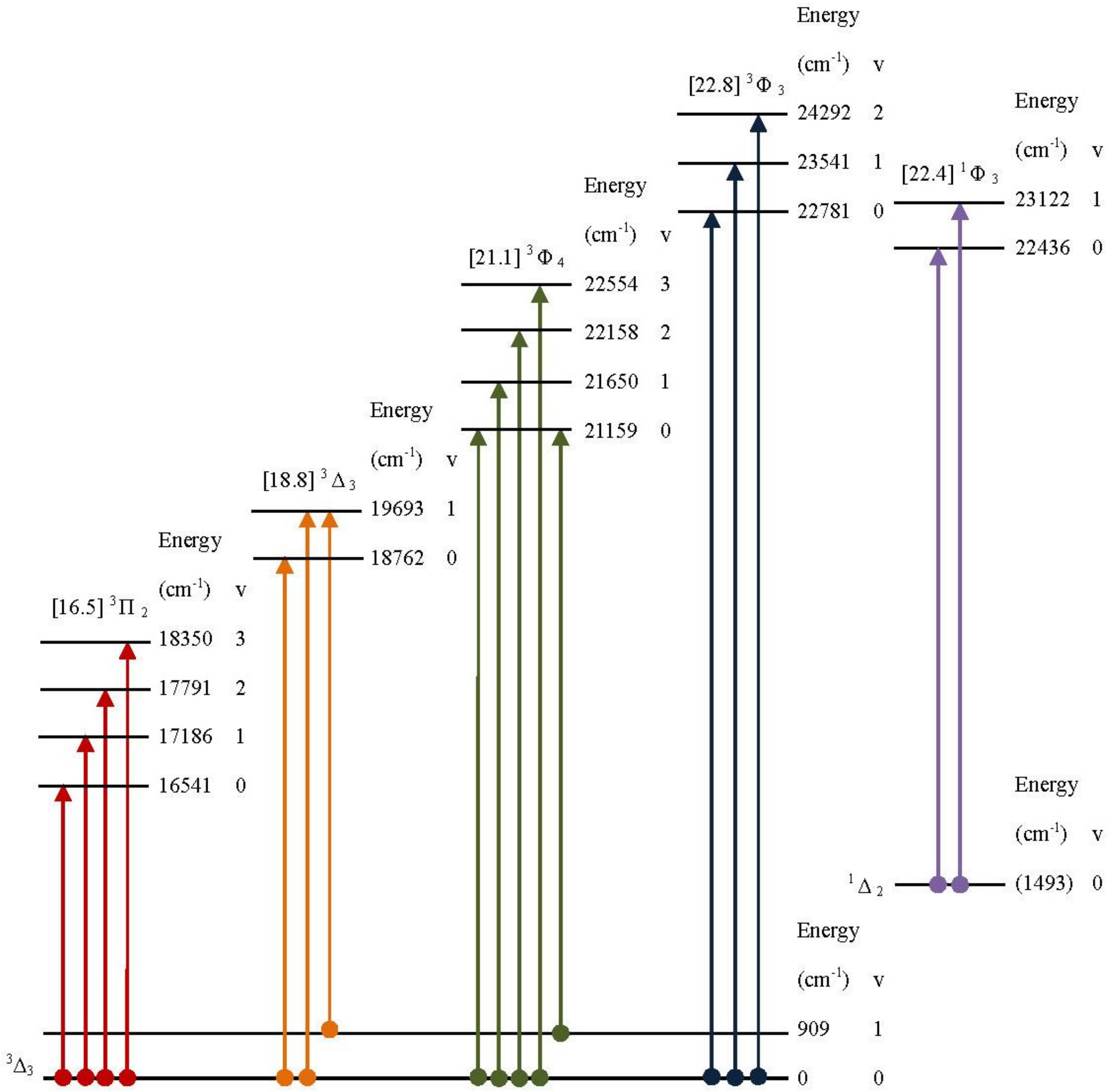
Energy
(cm^{-1}) v
[16.5] $^3\Pi_2$
18350 3
17791 2
17186 1
16541 0
Energy
(cm^{-1}) v
[18.8] $^3\Delta_3$
19693 1
18762 0
Energy
(cm^{-1}) v
[21.1] $^3\Phi_4$
22554 3
22158 2
21650 1
21159 0
Energy
(cm^{-1}) v
[22.8] $^3\Phi_3$
24292 2
23541 1
22781 0
Energy
(cm^{-1}) v
[22.4] $^1\Phi_3$
23122 1
22436 0
Energy
(cm^{-1}) v
$^1\Delta_2$
(1493) 0
Energy
(cm^{-1}) v
909 1
$^3\Delta_3$
0 0

Figure 3

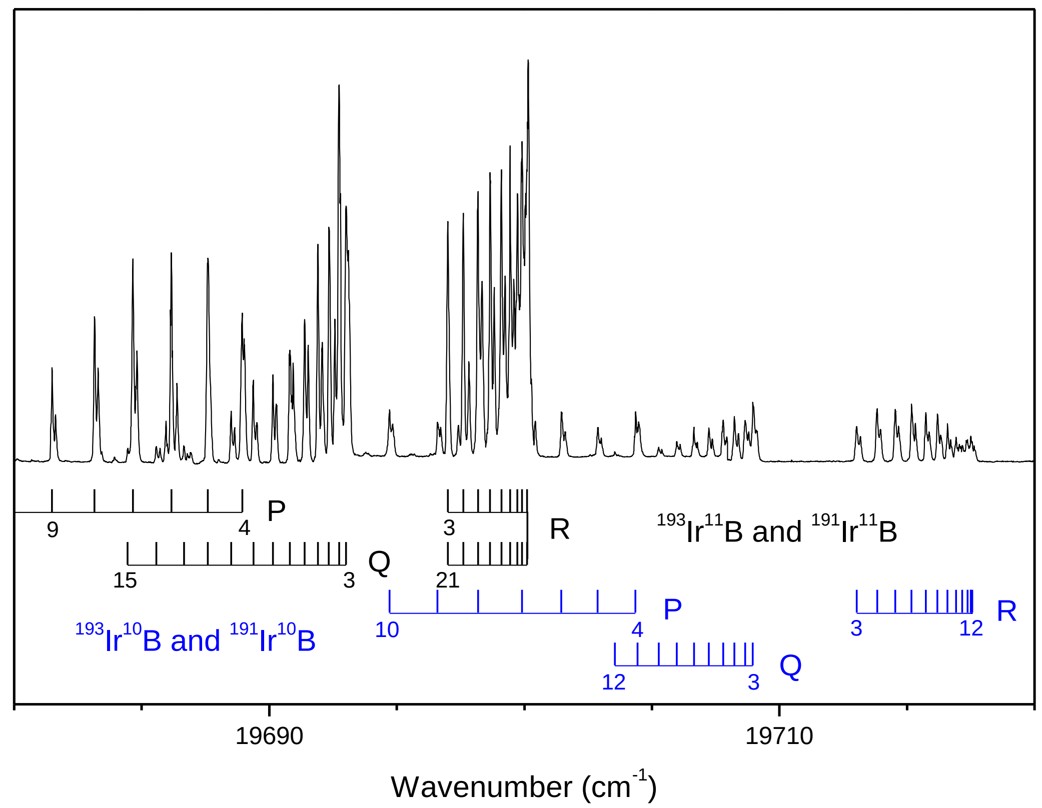
P
9
4
R
3
21
Q
15
3
^{193}Ir^{11}B and ^{191}Ir^{11}B
P
10
4
R
3
12
Q
12
3
^{193}Ir^{10}B and ^{191}Ir^{10}B
19690
19710
Wavenumber (cm^{-1})

Figure 4

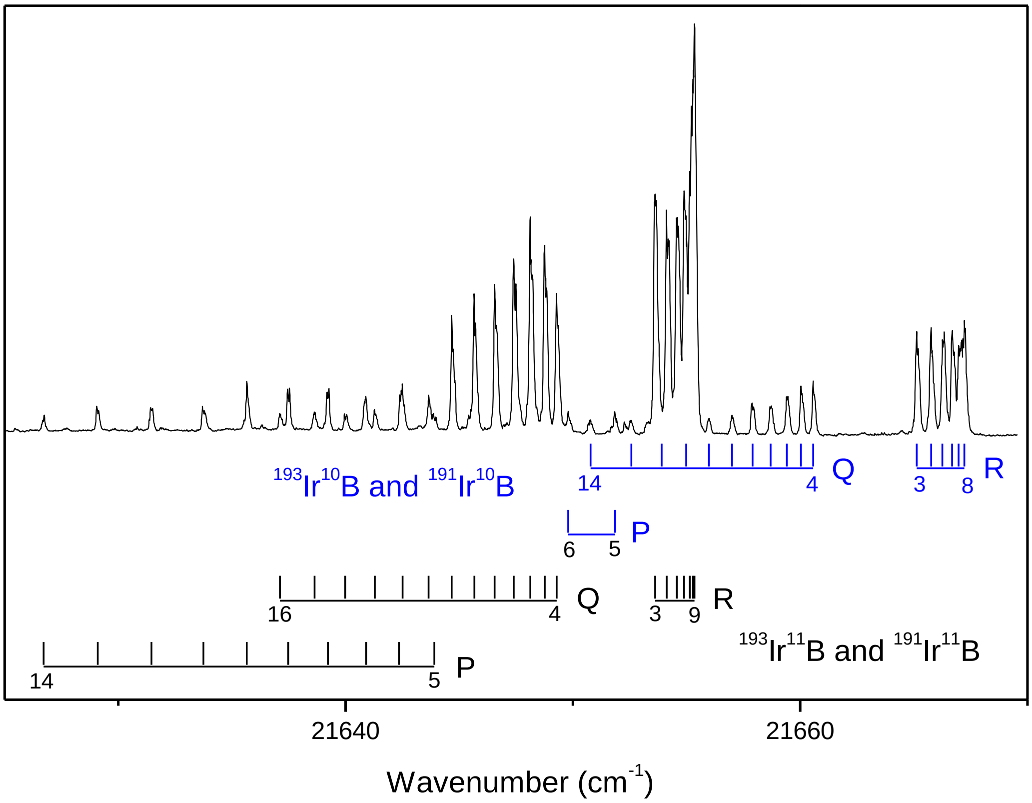

14
4
Q
3
8
R
^{193}Ir^{10}B and ^{191}Ir^{10}B
6
5
P
16
4
Q
3
9
R
^{193}Ir^{11}B and ^{191}Ir^{11}B
14
5
P
21640
21660
Wavenumber (cm^{-1})

Figure 5

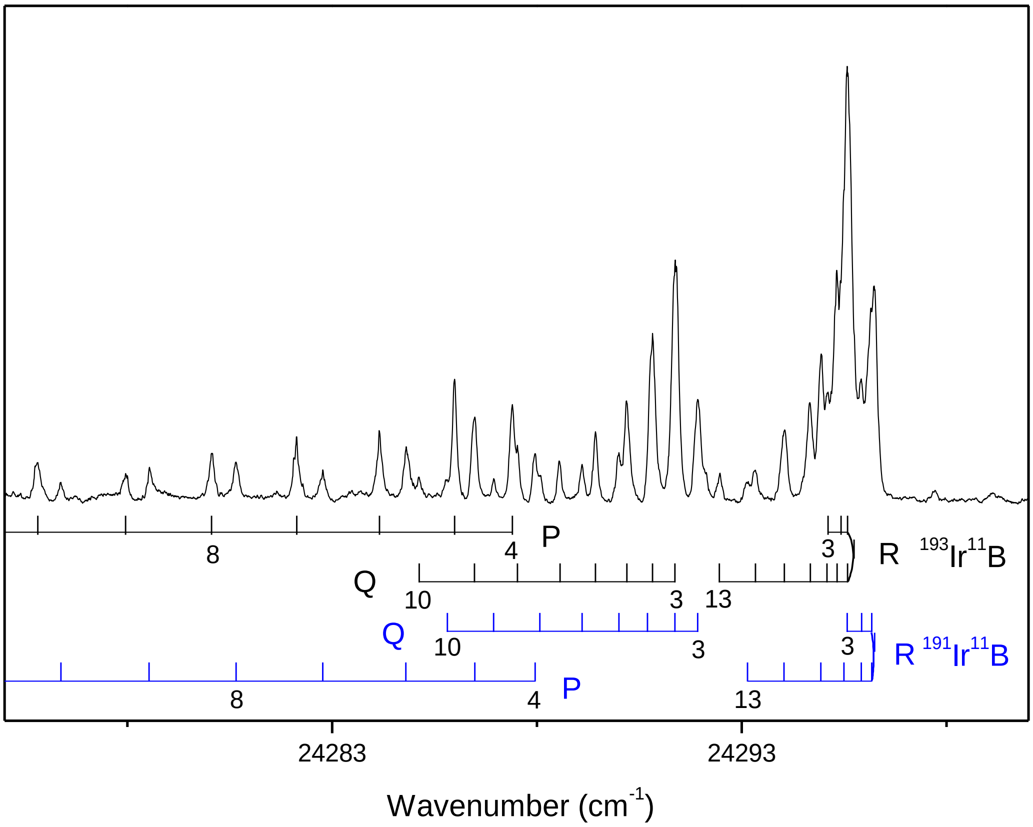
P
8
4
3
R
^{193}Ir^{11}B
Q
10
3
13
Q
10
3
3
R ^{191}Ir^{11}B
8
4
P
13
24283
24293
Wavenumber (cm^{-1})

Figure 6

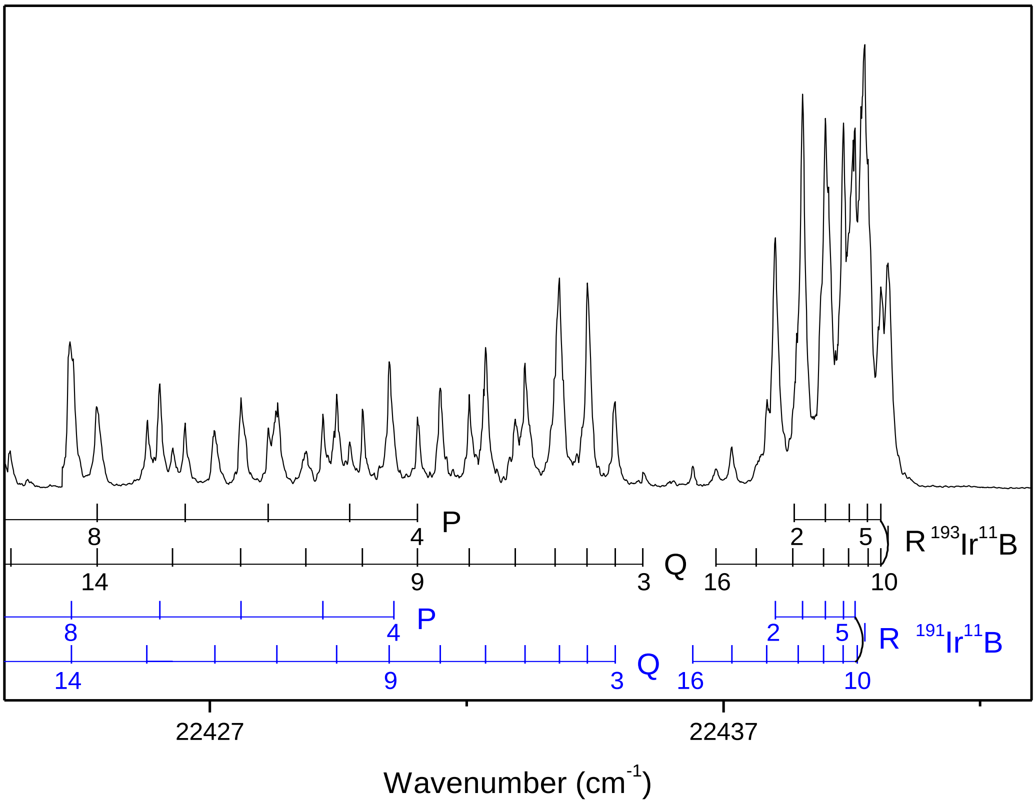

P
8
4
R ^{193}Ir^{11}B
2
5
Q
14
9
3
16
10
P
8
4
R ^{191}Ir^{11}B
2
5
Q
14
9
3
16
10
22427
22437
Wavenumber (cm^{-1})

^{191}Ir^{10}B and ^{193}Ir^{10}B

Assigned rotational lines of the [18.8] $^3\Delta_3$ – X $^3\Delta_3$ transition

	(0,0)		
J	P	Q	R
3		18759.76	18764.10
4	18755.10	18759.74	18765.06
5	18753.77	18759.41	18765.96
6	18752.48	18759.26	18766.96
7	18751.29*	18759.02	18767.94
8	18750.02	18758.74	18768.97
9	18748.69	18758.47	18769.78
10	18747.36	18758.20	18770.63
11	18746.01		18771.35
12	18744.47		18772.02
13	18742.87		18772.78*
14	18741.23		18773.42*
15			18774.09*
16			18774.69*

^{191}Ir^{11}B and ^{193}Ir^{11}B

Assigned rotational lines of the [18.8] $^3\Delta_3$ – X $^3\Delta_3$ transition

	(0,0)		
J	P	Q	R
3		18761.48	18765.41
4	18757.48	18761.40	18766.31
5	18756.24	18761.29	18767.20
6	18754.94	18761.14	18768.16
7	18753.66	18760.96	18769.06
8	18752.48	18760.75	18769.92
9	18751.29*	18760.52	18770.70
10	18750.07	18760.23	18771.43
11	18748.80		18772.14
12	18747.52		18772.78*
13	18746.22		18773.42*
14	18744.79		18774.09*
15	18743.32		18774.69*
16	18741.78		18775.21

* indicate overlapped with another line

$^{191}Ir^{10}B$

Assigned rotational lines of the [18.8] $^3\Delta_3 - X\ ^3\Delta_3$ transition

(1,0)

J	P	Q	R
3		19709.10	19713.17
4	19704.49	19708.80	19713.96
5	19703.02	19708.39	19714.67
6	19701.61	19707.94	19715.34
7	19700.05	19707.37	19715.87
8	19698.35	19706.77	19716.33
9	19696.74	19706.11	19716.71
10	19694.84	19705.40	19717.06
11		19704.52	19717.32
12			19717.55
13			19717.67*
14			19717.67*

$^{193}Ir^{10}B$

Assigned rotational lines of the [18.8] $^3\Delta_3 - X\ ^3\Delta_3$ transition

(1,0)

J	P	Q	R
3		19708.96	19713.03
4	19704.36	19708.65	19713.83
5	19702.88	19708.23	19714.54
6	19701.45	19707.80	19715.18
7	19699.91	19707.24	19715.74
8	19698.18	19706.65	19716.20
9	19696.59	19705.97	19716.59
10	19694.72	19705.27	19716.93
11		19704.43	19717.17
12		19703.55	19717.37
13			19717.50*
14			19717.55
15			19717.50*

* indicate overlapped with another line

$^{191}Ir^{11}B$

Assigned rotational lines of the [18.8] $^3\Delta_3$ – X $^3\Delta_3$ transition

(1,0)

J	P	Q	R
3		19693.11	19697.00
4		19692.79	19697.82*
5	19687.60*	19692.57	19698.35*
6	19686.38	19692.08	19698.82*
7	19684.82	19691.53	19699.25*
8	19683.29	19690.94	19699.59*
9	19681.62	19690.28	19699.91*
10	19679.83	19689.52	19700.10
11	19677.98	19688.64	19700.15*
12	19676.16	19687.60*	19700.15*
13	19674.17*	19686.79	19700.15*
14	19672.34	19685.72	19700.05
15	19670.07	19684.65	19699.91*
16	19668.06		19699.59*
17	19665.68		19699.25*
18	19663.41		19698.82*
19			19698.35*
20			19697.82*

* indicate overlapped with another line

$^{193}Ir^{11}B$

Assigned rotational lines of the [18.8] $^3\Delta_3 - X\ ^3\Delta_3$ transition

		(1,0)	
J	P	Q	R
3		19693.01	19697.00*
4	19688.94	19692.74	19697.60*
5	19687.60*	19692.34	19698.18*
6	19686.16	19691.91	19698.65*
7	19684.65	19691.39	19699.10*
8	19683.15	19690.81	19699.44*
9	19681.48	19690.15	19699.73*
10	19679.68	19689.38	19699.91*
11	19677.86	19688.51	19700.10*
12	19676.04	19687.60*	19700.15
13	19674.17*	19686.66	19700.10*
14	19672.05	19685.57	19699.91*
15	19669.94	19684.44	19699.73*
16	19667.94		19699.44*
17	19665.55		19699.10*
18	19663.29		19698.65*
19			19698.18*
20			19697.60*
21			19697.00*

* indicate overlapped with another line

^{191}Ir^{11}B and ^{193}Ir^{11}B

Assigned rotational lines of the [18.8] $^3\Delta_3 - X\ ^3\Delta_3$ transition

	(1,1)		
J	P	Q	R
3		18783.58	18787.35
4	18779.26	18783.36	18787.99
5	18777.93	18783.00	18788.57
6	18776.57	18782.54	18789.07
7		18782.08	18789.53
8			18789.96

* indicate overlapped with another line

$^{191}Ir^{10}B$

Assigned rotational lines of the [21.1] $^3\Phi_4 - X^3\Delta_3$ transition

J	P	Q	R
		(0,0)	
3			21157.96*
4		21153.34*	21158.57*
5	21147.58*	21152.92*	21159.28
6	21146.16*	21152.40*	21159.98
7	21144.67*	21152.04*	21160.61*
8	21143.05	21151.46*	21161.09*
9	21141.23	21150.92*	21161.52*
10		21150.29*	21161.87*
11			21162.15*
12			21162.36
13			21162.54

$^{193}Ir^{10}B$

Assigned rotational lines of the [21.1] $^3\Phi_4 - X\ ^3\Delta_3$ transition

J	P	Q	R
		(0,0)	
3			21157.96*
4		21153.34*	21158.57*
5	21147.58*	21152.92*	21159.20
6	21146.16*	21152.40*	21159.91
7	21144.67*	21152.04*	21160.61*
8	21142.97	21151.46*	21161.09*
9	21141.11	21150.92*	21161.52*
10		21150.29*	21161.87*
11			21162.15*
12			21162.36*
13			21162.51

* indicate overlapped with another line

$^{191}Ir^{11}B$

Assigned rotational lines of the [21.1] $^3\Phi_4 - X^3\Delta_3$ transition

	(0,0)		
J	P	Q	R
3			21163.08
4		21158.78*	21163.75*
5	21153.34	21158.43*	21164.36
6	21152.19	21157.96*	21164.93*
7	21150.69	21157.53	21165.45
8	21149.32	21156.96*	21165.86
9	21147.84*	21156.39	21166.19*
10		21155.74	21166.49*
11			21166.77*
12			
13			

$^{193}Ir^{11}B$

Assigned rotational lines of the [21.1] $^3\Phi_4 - X\ ^3\Delta_3$ transition

	(0,0)		
J	P	Q	R
3			21163.10
4		21158.78*	21163.75*
5	21153.33	21158.43*	21164.17
6	21152.04	21157.96*	21164.93*
7	21150.61	21157.49	21165.41
8	21149.23	21156.96*	21165.81
9	21147.84*	21156.32	21166.19*
10		21155.64	21166.49*
11			21166.77*
12			
13			

* indicate overlapped with another line

$^{191}Ir^{11}B$

Assigned rotational lines of the [21.1] $^3\Phi_4$ – X $^3\Delta_3$ transition

	(0,1)		
J	P	Q	R
3			20253.09
4		20249.08*	20253.81
5	20243.66	20248.72	20254.47
6	20242.35	20248.32	20255.06
7	20241.00	20247.84	20255.63
8	20239.64	20247.33	20256.09
9	20238.19	20246.70	20256.54
10	20236.69		20256.92
11			20257.27
12			20257.54*
13			

$^{193}Ir^{11}B$

Assigned rotational lines of the [21.1] $^3\Phi_4$ – X $^3\Delta_3$ transition

	(0,1)		
J	P	Q	R
3			20253.35
4		20249.08*	20254.05
5	20243.93	20248.78	20254.69
6	20242.60	20248.45	20255.32
7	20241.26	20248.04	20255.85
8	20239.88	20247.60	20256.36
9	20238.44	20247.07	20256.80
10	20236.95		20257.19
11			20257.54*
12			20257.77
13			20258.02
14			20258.25
15			20258.32

* indicate overlapped with another line

$^{191}Ir^{10}B$

Assigned rotational lines of the [21.1] $^3\Phi_4 - X\ ^3\Delta_3$ transition

(1,0)			
J	P	Q	R
3			21665.19
4		21660.65	21665.82
5		21660.10	21666.34
6		21659.45	21666.77
7	21651.92	21658.74	
8	21649.88	21657.95	
9		21657.06	

$^{193}Ir^{10}B$

Assigned rotational lines of the [21.1] $^3\Phi_4 - X\ ^3\Delta_3$ transition

(1,0)			
J	P	Q	R
3			21665.13
4		21660.57	21665.76
5		21660.03	21666.26
6		21659.40	21666.69
7	21651.85	21658.67	
8	21649.79	21657.88	
9		21657.00	

* indicate overlapped with another line

$^{191}Ir^{11}B$

Assigned rotational lines of the [21.1] $^3\Phi_4 - X^3\Delta_3$ transition

(1,0)			
J	P	Q	R
3			21653.65
4		21649.34	21654.20
5	21643.87	21648.85*	21654.65
6	21642.50*	21648.21*	21654.98*
7	21640.89	21647.50*	21655.21
8	21639.27*	21646.64	21655.31
9	21637.53*	21645.71*	21655.35*
10	21635.65*	21644.73	
11	21633.79	21643.65*	
12	21631.52	21642.50*	
13	21629.14	21641.36	
14	21626.74	21640.06*	
15	21624.42*		

$^{193}Ir^{11}B$

Assigned rotational lines of the [21.1] $^3\Phi_4 - X\ ^3\Delta_3$ transition

(1,0)			
J	P	Q	R
3			21653.62
4		21649.28	21654.12
5	21643.97	21648.85*	21654.60
6	21642.50*	21648.21*	21654.98*
7	21640.90	21647.50*	21655.14
8	21639.27*	21646.55	21655.29
9	21637.53*	21645.71*	21655.35*
10	21635.65*	21644.67	
11	21633.70	21643.65*	
12	21631.51	21642.50*	
13	21629.13	21641.27	
14	21626.74*	21640.06*	
15	21624.42*	21638.64	
16	21621.92	21637.11	

* indicate overlapped with another line

$^{191}Ir^{10}B$

Assigned rotational lines of the [21.1] $^3\Phi_4 - X\ ^3\Delta_3$ transition

(2,0)			
J	P	Q	R
3			22189.97
4		22185.55	22190.51
5	22179.97	22185.00	22190.98
6	22178.28*	22184.36	22191.35*
7	22176.37*	22183.58	22191.61*
8	22174.51	22182.69	
9	22172.62	22181.74	
10	22170.11	22180.70	
11			
12		22178.28*	

$^{193}Ir^{10}B$

Assigned rotational lines of the [21.1] $^3\Phi_4 - X\ ^3\Delta_3$ transition

(2,0)			
J	P	Q	R
3			22189.77
4		22185.36	22190.33
5	22179.28	22184.80	22190.77
6	22177.89*	22184.16	22191.10
7	22176.37*	22183.37	22191.35*
8	22174.21	22182.48	22191.61*
9	22171.99	22181.51	
10	22170.04	22180.58	
11			
12		22177.89*	

* indicate overlapped with another line

^{191}Ir^{11}B

Assigned rotational lines of the [21.1] $^3\Phi_4 - X\ ^3\Delta_3$ transition

(2,0)			
J	P	Q	R
3			22161.45
4		22157.32	22161.93
5	22151.73	22156.73	22162.35*
6	22150.18	22156.02	22162.57
7	22148.54	22155.21	22162.83*
8	22147.00	22154.30	22162.83*
9	22145.05	22153.28	
10	22143.17	22152.17	
11	22141.16	22151.00	
12	22138.96	22149.74	

^{193}Ir^{11}B

Assigned rotational lines of the [21.1] $^3\Phi_4 - X\ ^3\Delta_3$ transition

(2,0)			
J	P	Q	R
3			22161.21
4		22157.07	22161.71
5	22151.50	22156.47	22162.09
6	22149.96	22155.77	22162.35*
7	22148.33	22154.98	
8	22146.63	22154.05	
9	22144.85	22153.06	
10	22142.95	22152.94	
11	22140.93	22150.78	
12	22138.72	22149.52	

* indicate overlapped with another line

$^{191}Ir^{10}B$

Assigned rotational lines of the [21.1] $^3\Phi_4 - X\ ^3\Delta_3$ transition

	(3,0)		
J	P	Q	R
3			22583.90*
4		22579.34	22584.21*
5	22573.66*	22578.55	22584.28*
6	22571.28	22577.63	22584.28*
7	22569.21	22576.51	22584.21*
8	22567.05	22575.16	22583.90*
9	22564.85	22573.66*	
10	22562.35	22572.05	
11		22570.32	
12		22568.51	

$^{193}Ir^{10}B$

Assigned rotational lines of the [21.1] $^3\Phi_4 - X\ ^3\Delta_3$ transition

	(3,0)		
J	P	Q	R
3			22583.64
4		22579.21	22584.09*
5	22573.53*	22578.45	22584.21*
6	22571.18	22577.52	22584.28*
7	22569.10	22576.39	22584.09*
8	22566.95	22575.03	22583.90*
9	22564.74	22573.53*	
10	22562.33	22571.95	
11		22570.21	

* indicate overlapped with another line

$^{191}Ir^{11}B$

Assigned rotational lines of the [21.1] $^3\Phi_4 - X\ ^3\Delta_3$ transition

J	P	Q	R
		(3,0)	
3			22557.29*
4		22553.28	22557.77*
5	22548.06	22552.53	22557.99*
6	22546.29	22551.68	22557.99*
7	22544.50	22550.68	22557.99*
8	22542.62	22549.57	22557.64*
9	22540.60	22548.34	22557.29*
10		22546.97	22555.77*
11		22545.50	22554.74
12		22543.93	
13		22542.24	

$^{193}Ir^{11}B$

Assigned rotational lines of the [21.1] $^3\Phi_4 - X\ ^3\Delta_3$ transition

J	P	Q	R
		(3,0)	
3			22557.15
4		22553.14	22557.64*
5	22547.84	22552.40	22557.99*
6	22546.17	22551.55	22557.99*
7	22544.37	22550.55	22557.99*
8	22542.51	22549.44	22557.76
9	22540.37	22548.21	
10		22546.84	
11		22545.36	
12		22543.79	
13		22542.06	

* indicate overlapped with another line

^{191}Ir^{11}B and ^{193}Ir^{11}B

Assigned rotational lines of the [22.8] $^3\Phi_3 - X\ ^3\Delta_3$ transition

	(0,0)		
J	P	Q	R
3		22780.60	22784.48
4	22776.58	22780.14	22784.98
5	22775.13	22779.62	22785.46
6	22773.63	22779.01	22785.79
7	22772.05		22785.93
8	22770.24		

* indicate overlapped with another line

$^{191}Ir^{11}B$

Assigned rotational lines of the [22.8] $^3\Phi_3 - X\ ^3\Delta_3$ transition

	(1,0)		
J	P	Q	R
3		23540.61	23544.35
4	23536.49	23540.11	23544.81
5	23534.94*	23539.50	23545.06*
6	23533.31	23538.79	23545.31*
7	23531.62	23537.95	23545.39
8	23529.78	23537.06	23545.31*
9	23527.76	23536.04	23545.22
10	23525.60	23534.94*	23545.06*
11	23523.41		23544.51
12	23521.10		23544.08
13	23518.63		23543.56
14	23516.14		23542.81
15			23541.94

$^{193}Ir^{11}B$

Assigned rotational lines of the [22.8] $^3\Phi_3 - X\ ^3\Delta_3$ transition

	(1,0)		
J	P	Q	R
3		23540.31	23544.08
4	23536.20	23539.83	23544.51*
5	23534.66	23539.22	23544.81
6	23533.07	23538.51	23545.06*
7	23531.34	23537.69	23545.12*
8	23529.52	23536.80	23545.12*
9	23527.50	23535.76	23545.06*
10	23525.32		23544.73
11	23523.16		23544.35
12	23520.82		23543.88
13	23518.41		23543.26
14			23542.52
15			23541.65

* indicate overlapped with another line

$^{191}\mathrm{Ir}^{11}\mathrm{B}$

Assigned rotational lines of the [22.8] $^{3}\Phi_{3} - \mathrm{X}\ ^{3}\Delta_{3}$ transition

(2,0)			
J	P	Q	R
3		24291.92	24295.57
4	24287.95	24291.37	24295.90
5	24286.48	24290.70	24296.22*
6	24284.80	24290.00	24296.22*
7	24282.77	24289.10	24296.22*
8	24280.65	24288.07	24296.17
9	24278.53		24295.92
10	24276.38		24295.49
11	24274.11		24294.83
12	24271.73		
13	24269.02		

$^{193}\mathrm{Ir}^{11}\mathrm{B}$

Assigned rotational lines of the [22.8] $^{3}\Phi_{3} - \mathrm{X}\ ^{3}\Delta_{3}$ transition

(2,0)			
J	P	Q	R
3		24291.34	24295.10*
4	24287.40	24290.82	24295.42
5	24285.99	24290.19	24295.58*
6	24284.15	24289.43	24295.74
7	24282.13	24288.54	24295.58*
8	24280.05		24295.49
9	24277.95		24295.10*
10	24275.81		24294.67
11	24273.58		24294.04
12	24271.16		24293.33
13	24268.27		24292.45

* indicate overlapped with another line

$^{191}Ir^{11}B$

Assigned rotational lines of the [22.4] $^1\Phi_3 - a\ ^1\Delta_2$ transition

	(0,0)		
J	P	Q	R
2			22438.38
3		22435.46	22438.98
4	22431.05*	22434.89	22439.46
5	22429.72	22434.27	22439.80
6	22428.13	22433.73	22440.07
7	22426.52	22432.95	22440.21*
8		22432.05	22440.21*
9		22431.05*	22440.21*
10		22429.97	22440.07*
11			
12			
13			
14			22438.39
15			22437.73
16			22436.86

* indicate overlapped with another line

$^{193}Ir^{11}B$

Assigned rotational lines of the [22.4] $^1\Phi_3 - a\ ^1\Delta_2$ transition

(0,0)			
J	P	Q	R
2			22438.01
3			22438.54
4	22430.58	22434.35	22438.98
5	22429.20	22433.81	22439.34
6	22427.60	22433.14	22439.56
7	22426.03	22432.37	22439.75*
8		22431.49	22439.75*
9		22430.49	22439.70
10		22429.47	22439.52
11			22439.28
12			22438.90
13			22438.44
14			22437.85
15			22437.17
16			22436.41

* indicate overlapped with another line

$^{191}Ir^{11}B$

Assigned rotational lines of the [22.4] $^1\Phi_3 - a\ ^1\Delta_2$ transition

(1,0)

J	P	Q	R
2			23125.28
3		23121.95	23125.89*
4	23118.01	23121.55*	23126.39
5	23116.53	23121.17*	23127.00
6	23114.98	23120.57	23127.26
7	23113.45	23120.01	23127.41
8	23111.74	23119.21	
9		23118.41	

$^{193}Ir^{11}B$

Assigned rotational lines of the [22.4] $^1\Phi_3 - a\ ^1\Delta_2$ transition

(1,0)

J	P	Q	R
2			23124.83
3		23121.55*	23125.42
4	23117.52	23121.17*	23125.89*
5	23116.00	23120.70	23126.34
6	23114.43	23120.12	23126.70
7	23112.91	23119.48	23126.77
8	23111.22	23118.75	
9	23109.46	23117.89	
10	23107.54		

* indicate overlapped with another line